Computational Identification of Indole Alkaloids as Novel Hsp90 ATPase Inhibitors with Anticancer Potential

Adam A. Aboalroub

adam.hgf@gmail.com

Al-Ahliyya Amman University

Research Article

Keywords: Hsp90 inhibitors, Indole alkaloids, Molecular docking, Anticancer drug discovery, ATPase activity

Posted Date: September 7th, 2025

DOI: https://doi.org/10.21203/rs.3.rs-7419782/v1

Additional Declarations: No competing interests reported.

Abstract

The ATPase activity of heat shock protein 90 (Hsp90) is crucial for stabilizing and regulating many oncogenic client proteins, thereby supporting cancer progression and tumor cell survival. Although several small-molecule inhibitors have demonstrated preclinical promise, their clinical use remains limited due to toxicity and moderate effectiveness, highlighting the need for new chemotypes with better therapeutic profiles. Indole alkaloids, a diverse group of natural compounds with wide-ranging biological activities—including anticancer, antimicrobial, and enzyme-inhibition effects—were explored here as potential Hsp90 ATPase inhibitors through an extensive computer-based approach. Molecular docking of natural-product derivatives showed strong binding affinities (–10.004 to –10.691 kcal/mol), favorable pharmacokinetic and toxicity predictions, and key interactions with catalytic residues Asp93, Lys58, Gly97, and Thr184. Physicochemical and ADME profiling further validated favorable drug-like properties, including adherence to key medicinal chemistry filters, acceptable solubility, moderate lipophilicity, high oral bioavailability, and no structural alerts. Several indole-alkaloid derivatives also exhibited off-target interactions with several kinases, indicating potential for polypharmacological anticancer effects but emphasizing the importance of selectivity profiling. Overall, this research presents indole alkaloids as promising Hsp90-targeted anticancer candidates. Additional mechanistic studies and preclinical validation are necessary to advance these compounds toward clinical development.

Introduction

Heat shock protein 90 (Hsp90) is a highly conserved, ATP-dependent molecular chaperone essential for the folding, maturation, stabilization, and activation of various client proteins [1]. These include kinases, transcription factors, steroid hormone receptors, and signaling molecules, all vital for maintaining cellular homeostasis, growth, and survival [2]. Generally, Hsp90 supports protein balance by aiding proper folding of its clients and preventing aggregation during cellular stress like heat shock, oxidative stress, and hypoxia [1]. Beyond normal functions, misregulation of Hsp90 is linked to many diseases [2–4]. In cancer, it is often overproduced in an active form that binds and stabilizes oncogenic proteins such as HER2, AKT, RAF, and mutant p53 [4, 5]. This stabilization promotes cancerous behaviors by supporting cell growth signals, inhibiting cell death, encouraging blood vessel formation, and enabling metastasis [1, 4]. Hsp90 also plays a role in neurodegenerative diseases such as Alzheimer's, Parkinson's, and Huntington's by affecting the fate of misfolded and aggregating proteins [6, 7]. Moreover, certain pathogens hijack Hsp90 to fold their virulence factors, highlighting its importance as a therapeutic target in both cancer and infectious diseases [8]. The justification for targeting Hsp90 in therapy rests on its critical role in maintaining the function of many oncogenic proteins. Blocking Hsp90 interrupts its chaperone cycle, leading to the degradation of client proteins via ubiquitin–proteasome pathways, which in turn disables multiple cancer-driving pathways simultaneously [9]. This broad action provides an advantage over kinase inhibitors that target only a single signaling pathway [4, 9, 10]. Most small-molecule Hsp90 inhibitors work by competitively binding to the N-terminal domain (NTD), which contains a highly conserved ATP-binding site crucial for chaperone activity [11–13]. Although first-generation inhibitors like geldanamycin derivatives show promising anticancer effects, their clinical use is restricted by toxicity at high doses, poor solubility, and limited bioavailability [14]. Therefore, ongoing research is essential to identify new chemical structures that can effectively inhibit Hsp90 with better pharmacokinetic properties and safety.

Indole alkaloids are a vast and chemically diverse group of natural products containing an indole moiety—a bicyclic structure made of a benzene ring fused to a pyrrole ring [15]. They originate biosynthetically from tryptophan through various enzymatic processes, leading to a wide array of chemical structures [16]. These alkaloids are found across multiple biological kingdoms, including plants, marine organisms, fungi, and bacteria. Indole alkaloids possess a wide range of biological activities, making them highly valuable in medicinal chemistry as pharmacophores [15, 16]. Many key drugs and lead compounds are derivatives of indole alkaloids, highlighting their therapeutic importance [15]. Examples include vincristine and vinblastine (microtubule inhibitors for cancer treatment), camptothecin derivatives (topoisomerase I inhibitors), and reserpine (used for hypertension and psychosis) [17]. Their bioactivities span anticancer, antibacterial, antiviral, antifungal, antiparasitic, anti-inflammatory, and neuroactive effects [15–17]. In cancer therapy, indole alkaloids often work by disrupting essential cellular processes like microtubule assembly, DNA replication, and the cell cycle [16–18]. Their high affinity for various biological targets stems from the indole ring's ability to engage in π–π stacking, hydrogen bonds, and hydrophobic interactions, allowing recognition by numerous enzymes and receptors [16]. As pharmacophores, they exhibit remarkable structural flexibility, enabling modifications to improve potency, selectivity, and pharmacokinetic profiles [15–18]. The planar aromatic system and electron-rich nitrogen help interactions with both hydrophobic and polar regions of target proteins [15, 16]. This versatility has led to extensive exploration in structure-based drug design, such as kinase inhibitors, protease inhibitors, and chaperone modulators [17]. Overall, their adaptability makes indole alkaloids promising candidates for targeting Hsp90, where rational modifications of the indole core and its substituents can optimize engagement of the ATP-binding site.

In this study, we used a comprehensive computational approach to explore indole alkaloid–based molecules as potential Hsp90 inhibitors. We conducted molecular docking, ADMET predictions, and off-target and cytotoxicity predictions to evaluate their binding strength, pharmacokinetic features, and stability within the Hsp90 binding site. This integrated strategy aims to identify promising indole alkaloid frameworks that could be further developed into effective and selective anticancer agents targeting Hsp90. Numerous indole-alkaloids were identified from various chemical compound databases as potential inhibitors of Hsp90 ATPase activity. These compounds show promising drug-like characteristics, favorable pharmacokinetic profiles, and cytotoxic effects. Their strong binding affinities, between -10.004 and -10.691 kcal/mol, indicate their potential for further development. Examination of their binding interactions highlights key hydrogen bonds and hydrophobic interactions with essential catalytic residues, such as Lys58, Gly97, and Thr184, supporting their role as Hsp90 inhibitors. Furthermore, these indole-alkaloids showed strong multi-cancer cytotoxicity, highlighting their potential as lead anticancer candidates. Collectively, these results suggest that indole-alkaloids could constitute a new chemotype for Hsp90-targeted cancer treatments. Additional mechanistic studies and preclinical testing are necessary to move these compounds toward clinical use.

Materials and Methods

2.1 Ligand Library Preparation

A targeted library of indole alkaloid–based molecules was assembled by gathering compounds from various public chemical and natural product databases, including ZINC (https://zinc.docking.org), Mcule (https://mcule.com), LOTUS Natural Products Database, PubChem (https://pubchem.ncbi.nlm.nih.gov), and relevant scientific literature. Selection criteria prioritized maximizing structural diversity and key pharmacophoric features. This meant focusing on compounds with an indole core and potential substituents that could engage in different interactions within the Hsp90 binding site. The initial compound set was curated to remove duplicates, inorganic species, and molecules over 500 Da. Additionally, the library was filtered using Lipinski's Rule of Five (Ro5), which states that an orally active drug generally has a molecular weight of 500 Da or less, a calculated LogP value not greater than 5, no more than five hydrogen bond donors (HBD), and no more than ten hydrogen bond acceptors (HBA) [19]. Compounds that violated more than one of these parameters were excluded, as such deviations are often linked to poor pharmacokinetic behavior, including limited absorption, distribution, metabolism, and excretion (ADME). This filtering step was essential to increase the chance of identifying bioavailable and pharmacologically active molecules suitable for further development. The shortlisted compounds were then converted into their SMILES (Simplified Molecular Input Line Entry System) representations, which served as input for subsequent computational analyses in the virtual screening workflow.

2.2 Molecular Docking

The N-terminal domain of human Hsp90 in complex with a co-crystallized inhibitor (PDB ID: 6LTI, 1.59 Å resolution) was obtained from the RCSB Protein Data Bank (https://www.rcsb.org) [20]. Protein preparation was carried out using AutoDock Tools (1.5.7) by removing water molecules, ions, and non-essential heteroatoms, and extracting the co-crystallized ligand to define the binding site [21]. Missing hydrogens were added, polar hydrogens included for hydrogen-bond calculations, and Gasteiger charges assigned; non-polar hydrogens were merged with their parent carbons. A grid box with a volume of 10 Å^3 and a default spacing of 0.375 Å was generated, centered at coordinates x = 33.00, y = -14.00, and z = -20.00, to define the docking search space. The actual docking simulations of the selected indole-alkaloids were performed using AutoDock Vina (1.2.3) with Sampling exhaustivity of 40. The resulting conformations were analyzed from the AutoDock log files, with emphasis placed on the lowest binding energy (LBE) values to identify the most favorable poses. To enhance reliability, the conformer with the largest cluster size was selected for further analysis. The final chosen conformers were exported and visualized using ChimeraX-1.8 [22].

2.3 In silico prediction of physicochemical properties, drug-likeness, and lead-likeness for the top-ranked molecules

The physicochemical properties, drug-likeness, and lead-likeness profiles of the top-ranked indole alkaloid molecules identified from docking studies were evaluated using SwissADME (http://www.swissadme.ch/) [23]. Compounds were first screened according to Lipinski's Rule of 5. Additional drug- and lead-likeness assessments were performed by applying medicinal chemistry filters, including the Veber (polar surface area ≤ 140 Å^2 and ≤ 10 rotatable bonds), Ghose (molecular weight 160–480 Da, logP −0.4 to +5.6, molar refractivity 40–130), and Egan (logP ≤ 5.88 and polar surface area ≤ 131 Å^2) rules, thereby providing a comprehensive evaluation of the compounds' oral bioavailability and suitability as potential leads.

2.4 In Silico Cytotoxicity Prediction in Tumor Cell Lines

Evaluating cytotoxicity in tumor cell lines is crucial in anticancer drug development, as it helps assess both therapeutic effectiveness and safety. Computational methods for predicting cytotoxicity provide a quick and cost-efficient alternative to laboratory testing, reducing resource use during early candidate screening. In this study, the cytotoxic potential of top-ranked indole alkaloid–based molecules was evaluated using CLC-Pred 2.0 (Cell Line Cytotoxicity Predictor), a web platform for *in silico* prediction of activity against cancerous and non-cancerous cell lines (https://www.way2drug.com/Cell-line) [24]. CLC-Pred 2.0 employs QSAR models trained on extensive experimental cytotoxicity datasets, predicting activity by correlating the compound's structural features with known bioactive molecules in its database. For each indole alkaloid derivative, the SMILES notation was generated and submitted to the CLC-Pred server. The results indicated the probability of cytotoxic activity across various tumor cell lines, aiding in the identification of candidates with the highest predicted anticancer potential for further investigation.

2.5 Off-Target Prediction

To assess the potential off-target effects of the top-ranked indole alkaloid compounds, an *in silico* screening was conducted using the Way2Drug PASS (Prediction of Activity Spectra for Substances) platform (http://www.way2drug.com/PASS) [25]. This tool predicts a wide range of biological activities, including both desired pharmacological effects and possible adverse or toxicological outcomes, based on structural similarity to known bioactive compounds. Each prediction is given as the probability of activity (Pa) versus inactivity (Pi), with higher Pa values indicating a greater likelihood that the compound will exhibit the predicted activity. For this study, activities with Pa > 0.7 were considered highly probable, while those with 0.5 < Pa < 0.7 were regarded as moderately probable. This method enabled the identification of potential off-target interactions, offering insights into the safety profile and pharmacological significance of the selected indole alkaloids.

Results

Computer-aided drug discovery (CADD) is a rapidly advancing field that helps identify and analyze molecules with desired biological effects [11, 13, 26–28]. Recent advances in computational chemistry and machine learning have significantly improved the accuracy of predicting and ranking chemical compounds for specific biological functions. In this study, we used *in silico* methods to find indole alkaloid–based molecules capable of inhibiting Hsp90 ATPase activity. Using bioactive small molecules to influence protein function is a promising approach for developing targeted anticancer therapies. Compared to larger therapeutics like monoclonal antibodies and polypeptides, small molecules offer advantages such as lower manufacturing costs, oral bioavailability, improved patient compliance, and favorable pharmacokinetics [29, 30]. They can also target various proteins, including kinases, proteasomes, and chaperones like Hsp90 [10, 31, 32]. This research employed virtual screening and molecular docking to identify diverse indole alkaloid scaffolds with high binding affinity and firm interaction profiles at the Hsp90 ATP-binding site. These computational findings serve as a valuable initial step in drug discovery,

highlighting promising candidates for biological activity. However, confirming the therapeutic potential of these compounds will require further validation through in vitro biochemical tests, cell-based cytotoxicity assessments, and detailed pharmacokinetic and pharmacodynamic studies.

3.1 Ligand Library Preparation and Shortlisting

A diverse library of indole alkaloid–based molecules was compiled from public databases such as ZINC, Mcule, LOTUS, and PubChem, along with relevant literature. The selection prioritized maintaining the indole core while adding substituents capable of hydrogen bonding, hydrophobic interactions, and ion–π stacking with Hsp90. The dataset was curated to eliminate duplicates, inorganic compounds, and molecules larger than 500 Da, ensuring drug-like properties. After initial structural optimization, a filtering process based on Lipinski's Ro5 was applied to favor bioavailable, pharmacologically relevant Hsp90 inhibitors. Compounds were evaluated for molecular weight (≤500 Da), cLogP (≤5), hydrogen bond donors (≤5), and acceptors (≤10). Those exceeding these thresholds were excluded, mainly due to high lipophilicity or molecular weight, reducing the initial 1,240 compounds to 812 (a 34.5% reduction). This improved dataset suited molecular docking, focusing on scaffolds with balanced physicochemical properties to enhance binding potential and ADME profiles. The filtered compounds were converted into SMILES format for subsequent computational analyses.

3.2 Evaluation of Indole Alkaloid–Based Molecules as Potential Hsp90 Inhibitors via Molecular Docking

After assembling the indole alkaloid library, compounds that did not meet Lipinski's Rule of Five were removed, and the remaining molecules underwent molecular docking against the Hsp90 N-terminal domain (PDB ID: 6LTI). Binding affinities were estimated as docking scores (ΔG, kcal/mol), and compounds were ranked based on these scores, with more negative values indicating stronger predicted binding. As shown in Table 1 and depicted in Figure 1, a subset of ligands had docking scores of ≤ –10.0 kcal/mol, indicating strong binding potential and good complementarity to the Hsp90 active site. Notably, the top ten compounds showed a narrow energy range (–10.691 to –10.004 kcal/mol), reflecting consistently high predicted affinity for the ATP-binding pocket. The LBE value derived from molecular docking is used to gauge binding strength: values more negative than –10.0 kcal/mol are considered strong binders, those between –9.0 and –10.0 kcal/mol are moderate binders, while values less negative than –9.0 kcal/mol typically indicate weak binding affinity [33].

Table 1. Top 10 ranked indole alkaloid–based molecules docked into the Hsp90 ATP-binding site, with their predicted docking scores, molecular weights, and SMILES strings.

Rank	PubChem CID	Docking Score (kcal/mol)	SMILES
1	4200841	-10.691	C1OC2=C(O1)C=C(C=C2)C(C3=CNC4=CC=CC=C43)C5=CNC6=CC=CC=C65
2	2940578	-10.119	C1(C2=CC=CC=C2NC=1)C(C1C=CC(=C(OC)C=1)OCC(O)=O)C1C2C=CC=CC=2NC=1
3	24718647	-10.109	C12=CC(CNC(CC(C3C=CC4OCOC=4C=3)C3C4C=CC=CC=4NC=3)=O)=CC=C1OCO2
4	2924030	-10.038	C1(C2=CC=CC=C2NC=1)C(C1C=CC=C(C)C=1O)C1C2C=CC=CC=2NC=1
5	2940798	-10.015	C1(C2=CC=CC=C2NC=1)C(C1C=CC=C(C=1)N(=O)=O)C1C2C=CC=CC=2NC=1
6	2923908	-10.012	C1(C2=CC=CC=C2NC=1)C(C1C=C(OC)C=CC=1O)C1C2C=CC=CC=2NC=1
7	4292821	-10.010	C1(C2=CC=CC=C2NC=1)C(C1C=CC(=CC=1)C(O)=O)C1C2C=CC=CC=2NC=1
8	2949399	-10.009	C1(C2=CC=CC=C2N(C)C=1)C(C1C=CC(=CC=1)O)C1C2C=CC=CC=2N(C)C=1
9	2923935	-10.007	C1(C2=CC=CC=C2NC=1)C(C1C=CC=C(OCC)C=1O)C1C2C=CC=CC=2NC=1
10	2949436	-10.004	C1(C2=CC=CC=C2N(C)C=1)C(C1C=CC=NC=1)C1C2C=CC=CC=2N(C)C=1

All top-ranking hits shared a 3,3'-di(indolyl)methane-like (DIM) scaffold, composed of two indole- or carbazole-type aromatic systems connected by a central carbon atom (Figure 2A). This conjugated π-surface enabled extensive hydrophobic and cation-π interactions, supported by limited hydrogen-bonding capability from the indole NH group (absent in N-methylated analogues). In control docking, ATP adopted the expected binding pose—anchored within the adenine sub-pocket via backbone hydrogen bonds, with its triphosphate group extending toward the solvent-exposed phosphate-binding region (Figure 2B). Similarly, the DIM core aligned within the canonical ATP-binding pocket, overlapping with the adenine-binding region (Figure 2B–D) [34, 35]. The central linking carbon positioned the fused aromatic systems parallel to the pocket's hydrophobic wall, facilitating multiple interactions with non-polar residues (Figure 2E). Typically, one indole ring occupied the adenine sub-pocket, while the second extended toward the pocket entrance, where substituents such as phenol, methoxy, benzodioxole, or carboxylate groups interacted with polar residues and solvent-exposed features at the rim.

Despite the structural diversity at these peripheral positions, docking scores for DIM derivatives remained closely grouped, emphasizing the dominant role of the scaffold's hydrophobic and cation-π interactions in driving binding. Substituents such as phenol, methoxy, nitro, carboxylic acid, and benzodioxole were all well tolerated, with minimal loss of predicted affinity. Significantly, N-methylation of the indole nitrogen (CIDs 2949399 and 2949436) did not reduce docking scores, indicating that the indole NH is not essential for target engagement. The top-ranked compound (CID 4200841, ΔG = –10.691 kcal/mol) featured a benzodioxole substituent, likely improving shape complementarity and providing additional hydrogen-bond acceptor sites at the binding pocket edge. Similarly, derivatives with polar acidic groups, such as CID 4292821 with a benzoic acid group, maintained strong affinities, possibly through salt-bridge formation—though such groups might affect membrane permeability. Nitro-substituted analogues (e.g., CID 2940798) kept docking performance but raised concerns about mutagenicity and metabolic stability. Flexible substituents, such as the phenoxyethyl linker in CID 2923935, offered no advantage over more rigid analogues, suggesting that the Hsp90 binding pocket prefers compact, rigid aromatic systems. Overall, the SAR from these docking studies highlights

the DIM scaffold as a key core for Hsp90 binding, with peripheral modifications acting as modulators of solubility, permeability, and selectivity. The tolerance for both hydrogen-bond donors (phenol) and acceptors (methoxy, pyridine) at the pocket entrance shows that polar interactions can be strategically used to adjust ligand orientation and pharmacokinetics without disrupting core binding. Future optimization should focus on rigid aromatic substituents to enhance shape fit, replace metabolically unstable or toxic groups (e.g., nitro), and incorporate bioisosteres for acidic functionalities—aiming to improve drug-like properties while maintaining high affinity.

Docking analysis of Hsp90 NTD showed that indole-alkaloids bind in ways similar to typical ATP-site inhibitors. Most compounds formed consistent hydrogen bonds with Asp93, Gly97, Asn51, and Thr109 (Table 2), which are crucial for anchoring nucleotides in the adenine-binding pocket [36]. Additional stabilizing interactions involved Ser52, Ser50, Thr184, and sometimes backbone contacts with Gly137, while Phe138 was mainly stabilized through aromatic stacking. A preserved hydrophobic cluster—including Leu107, Met98, Ala55, Gly108 (backbone), and Thr109—helped support the indole core and its groups, further strengthening binding stability.

Table 2: Key Residues of Hsp90 Involved in Indole-Alkaloid Interactions

PubChem CID	Interactions			
	H-Bonds	Hydrophobic	ion-π	Ionic
4200841	Thr109, Asn51, Gly97, Asp93, Ser52	Gly97, Gly108, Asn51, Lys58, Ala55, Thr184, Leu107	Lys58	-
2940578	Asp93, Ser52, Gly97, Asn51, Phe138, Gly137	Gly137, Phe138, Asn51, Gly97, Asp93, Se52	-	-
24718647	Thr109, Ser50, Lys58, Thr109, Asn51, Asp93, Thr184, Gly135	Asn51, Met98, Gly108, Gly97, Leu107, Ser50, Thr108	-	-
2924030	Gly97, Leu107, Thr109, Ser50, Asp93, Gly108	Leu107, Asn51, Asp54, Gly97, Lys58, Thr109, Met98	Lys58	-
2940798	Asn51, Phe138, Thr109, Gly97, Asp93	Met98, Leu107, Thr109, Asn51, Gly97, Asp54	Lys58	-
2923908	Thr109, Asp54, Asn51, Asp93, Gly97, Ala55	Leu107, Gly97, Ala55, Thr184, Gly108, Asp54	Lys58	-
4292821	Thr109, Ser50, Asp54, Ser52, Asp93, Gly97	Asp93, Ser52, Gly97, Thr109, Ala55, Asp54	Lys58	His154
2949399	Gly97, Lys58, Ile96	Gly109, Leu107, Asn51, Lys58, Met98	Lys58	-
2923935	Gly108, Thr109, Asp93, Gly97	Asp54, Leu107, Gly97, Thr109, Phe138	Lys58	-
2949436	Lys58, Thr109, Gly108	Asp54, Phe138, Leu107, Gly108, Asn51	-	-

A prominent feature across most ligands was the engagement of Lys58 in ion–π interactions with the indole ring, observed in eight of the ten top compounds (Figure 3D–E). This emphasizes the central role of the indole scaffold in stabilizing binding. Two ligands (CIDs 2940578 and 2949436) lacked Lys58-mediated contacts but compensated through extensive hydrogen-bond networks involving Asp93, Gly97, Asn51, and Ser52, highlighting alternative strategies for high-affinity binding. Unique binding features were also observed. CID 4292821 (Rank 7) not only formed typical hydrogen bonds with Thr109, Asp93, Gly97, and Ser52, and hydrophobic contacts with Ala55, Leu107, and Asp93, but also engaged His154 via its carboxylate group (Figure 3F). Since His154 is not commonly involved in ATP-site recognition, this suggests that CID 4292821 adopts a deeper or altered orientation, exploiting an underutilized region of the pocket. This interaction underscores the chemical flexibility of indole-alkaloids and presents opportunities to design derivatives with increased selectivity. Comparisons among ligands revealed distinct binding preferences. CID 24718647 exhibited the broadest network of interactions, engaging eight residues through hydrogen bonds and hydrophobic contacts, indicating a very stable fit. In contrast, CID 2949399 achieved strong affinity despite fewer hydrogen bonds, relying mainly on compact hydrophobic interactions with Leu107, Met98, and Gly109. The top-ranked compound, CID 4200841, combined extensive hydrogen bonding (Asp93, Gly97, Ser52, dioxole oxygens) with hydrophobic contacts (Leu107, Thr184, Gly108, Ala55, Asn51), along with a stabilizing Lys58 ion–π interaction. Similarly, CID 2940578 achieved strong binding through multiple hydrogen bonds (Asp93, Gly97, Ser52, Asn51, Gly137, Phe138) and complementary hydrophobic stabilization. CID 24718647 further demonstrated a rich interaction profile, with its amide group engaging Asn51, Thr109, and Gly135, while its dioxole substituents contacted Lys58, Ser50, and Met98, enhancing stability through both polar and hydrophobic contributions. These findings align with established Hsp90 inhibitors. Classical inhibitors such as geldanamycin and ansamycin derivatives depend on Asp93 and Gly97, while purine-based scaffolds like PU-H71 mimic the adenine ring through interactions with Asp93 and Asn51. Indole-alkaloids not only replicate these canonical interactions but also introduce new features—particularly Lys58-mediated ion–π contacts absent in most purine analogs, and in the case of CID 4292821, a novel ionic interaction with His154. In summary, indole-alkaloids serve as potent ATP-competitive inhibitors of Hsp90 NTD. Their high predicted affinities come from conserved hydrogen bonds (Asp93, Gly97, Asn51, Thr109), hydrophobic stabilization within the Leu107–Met98–Ala55 cluster, and frequent ion–π interactions with Lys58. The unique His154 interaction observed for CID 4292821 broadens the pharmacophoric landscape of the ATP pocket, suggesting that rationally designed indole derivatives could target underexplored residues to achieve enhanced potency and selectivity.

3.3 Physicochemical and Drug-Likeness Properties of Indole-Alkaloids Predicted by SwissADME

Physicochemical profiling of the selected indole-alkaloid compounds was conducted using various drug-likeness and lead-likeness criteria (Table 3). The molecular weights (MW) of the compounds ranged from 351.44 to 442.46 Da, all below the 500 Da threshold specified by Lipinski's Ro5 for oral bioavailability [19]. The number of rotatable bonds varied from 3 to 7, within the Veber guideline limit (≤10), which favors molecular flexibility and absorption [37]. HBA ranged from 1 to 5, and HBD from 0 to 3, both within recommended ranges for permeability and oral activity [19, 37]. The topological polar surface area (TPSA) values ranged from 22.75 to 87.87.34 Å², well below the 140 Å² limit, indicating potential for good membrane permeability and CNS penetration for the lower TPSA compounds (e.g., CID 2949436 with TPSA = 22.75 Å²) [38]. Lipophilicity, measured by consensus Log P, ranged from 3.88 to 4.80, indicating moderate to high hydrophobicity, which may enhance membrane crossing but could affect solubility [39]. The ESOL-predicted solubility (Log S)

values (-5.19 to −5.99) showed moderate solubility for all compounds, a common trait of hydrophobic scaffolds [39]. Drug-likeness evaluation confirmed that all compounds adhered to Lipinski's, Ghose's, Veber's, and Egan's rules, with only isolated violations in Ghose's or Egan's parameters for a few (e.g., CID 2940798 and CID 2923935). The Muegge filter flagged most compounds (except CID 24718647 and CID 2949436) with one violation, often related to hydrophobicity [23]. The bioavailability scores were generally high (0.55), with one compound (CID 4292821) scoring 0.85, indicating excellent oral bioavailability prospects [40]. No PAINS (Pan Assay Interference Compounds) or Brenk alerts were detected, suggesting low risk of assay interference or chemical reactivity issues. However, all compounds exhibited two lead-likeness violations related to molecular weight, many above 350, and increased hydrophobicity, which could hinder further optimization for smaller fragment-like leads [37]. Overall, these ADME and drug-likeness profiles suggest the investigated indole-alkaloids have favorable physicochemical properties for oral drug development [41, 42]. They show moderate lipophilicity, acceptable solubility, high compliance with medicinal chemistry filters, and no major structural alerts. Along with their predicted activity against Hsp90 NTD and promising cytotoxicity profiles, these features make them strong candidates for further refinement.

Table 3. Physicochemical and Drug-Likeness Properties of Indole-Alkaloids Predicted by SwissADME

PubChem CID	MW (g/mol)	#RB	HBA	HBD	TPSA	LogP	LogS	Solubility	Lipinski Violations	Ghose Violations	Veber Violations	Egan Violations	Muegge Violations
4200841	366.41	3	2	2	50.04	4.67	-5.92	Moderately soluble	0	0	0	0	1
2940578	426.46	7	4	3	87.34	4.2	-5.78	Moderately soluble	0	0	0	0	1
24718647	442.46	7	5	2	81.81	3.88	-5.19	Moderately soluble	0	0	0	0	0
2924030	352.43	3	1	3	51.81	4.78	-5.99	Moderately soluble	0	1	0	0	1
2940798	367.4	4	2	2	77.4	4.27	-5.88	Moderately soluble	0	1	0	1	1
2923908	368.43	4	2	3	61.04	4.39	-5.75	Moderately soluble	0	0	0	0	1
4292821	366.41	4	2	3	68.88	4.37	-5.68	Moderately soluble	0	0	0	0	1
2949399	366.45	3	1	1	30.09	4.5	-5.76	Moderately soluble	0	0	0	0	1
2923935	382.45	5	2	3	61.04	4.8	-5.98	Moderately soluble	0	1	0	1	1
2949436	351.44	3	1	0	22.75	4.21	-5.24	Moderately soluble	0	0	0	0	0

3.4 Cytotoxicity Prediction Analysis of Screened Indole-Alkaloids

CLC-Pred 2.0 was used to predict the cytotoxic potential of selected indole-alkaloid compounds against various human cancer cell lines [24]. The analysis revealed a range of predicted activities (Pa) and probabilities of inactivity (Pi), highlighting several compounds with strong potential anticancer effects (Table 4 and Figure 4). A compound was considered potentially active when Pa > 0.5 and higher than the corresponding Pi value. Compound CID 4200841 showed the highest predicted activity toward Hs 683 oligodendroglioma cells (Pa = 0.721, Pi = 0.008), suggesting strong anti-brain cancer potential. It also showed high predicted cytotoxicity against lung carcinoma cell lines DMS-114 (Pa = 0.570) and NCI-H460 (Pa = 0.545), alongside moderate activity for breast carcinoma MCF-7 (Pa = 0.544) and ovarian adenocarcinoma OVCAR-5 (Pa = 0.506). CID 2940578 showed a relatively selective effect on MCF-7 breast carcinoma (Pa = 0.582), while CID 24718647 exhibited moderate activity against NCI-H460 (Pa = 0.415). CID 2924030 demonstrated vigorous predicted activity on Hs 683 oligodendroglioma (Pa = 0.608) and moderate potential for NCI-H460 (Pa = 0.513). CID 2940798 showed moderate cytotoxicity toward NCI-H460 (Pa = 0.501). CID 2923908 had activity against both Hs 683 (Pa = 0.583) and NCI-H460 (Pa = 0.563), with additional potential against MCF-7 (Pa = 0.536). CID 4292821 also favored NCI-H460 (Pa = 0.543) and showed moderate activity for MCF-7 (Pa = 0.507). CID 2949399 emerged as a strong candidate for lung cancer cytotoxicity with the highest activity against NCI-H460 (Pa = 0.722, Pi = 0.005) and moderate activity for ovarian adenocarcinoma OVCAR-5 (Pa = 0.523) and MCF-7 (Pa = 0.509). CID 2923935 showed moderate potential against Hs 683 (Pa = 0.503). Notably, CID 2949436 was the most potent compound in the dataset, showing exceptional predicted activity toward NCI-H460 non-small cell lung carcinoma (Pa = 0.906, Pi = 0.004), PANC-1 pancreatic carcinoma (Pa = 0.710), ACHN papillary renal carcinoma (Pa = 0.704), and HCT-116 colon carcinoma (Pa = 0.616). Overall, the predicted profiles suggest that several indole-alkaloids, especially CID 2949436, 2949399, and 4200841, have significant anticancer potential with multiple targets across different cancer types. The frequent high activity against lung carcinoma cell lines (NCI-H460, DMS-114, A549) indicates possible structural features within these compounds that confer selectivity for pathways essential to lung cancer cell survival. The broad-spectrum activity of CID 2949436, covering lung, pancreas, kidney, and colon cancers, points to its potential as a lead scaffold for developing multi-cancer therapeutic agents. However, this widespread activity also requires careful assessment of off-target effects. These *in silico* results provide valuable leads for experimental validation, highlighting CID 2949436 for its

remarkable potency, along with CID 2949399 and CID 4200841 as promising candidates for further in vitro and in vivo studies targeting Hsp90 NTD-related anticancer mechanisms.

Table 4. Predicted cytotoxicity of Indole-alkaloids by CLC-Pred 2.0

Compound CID	Pa	Pi	Cell-line	Cell-line name	Tissue/organ
4200841	0.721	0.008	Hs 683	Oligodendroglioma	Brain
	0.570	0.015	DMS-114	Lung carcinoma	Lung
	0.545	0.015	NCI-H460	Non-small cell lung carcinoma	Lung
	0.544	0.043	MCF 7.00	Breast carcinoma	Breast
	0.540	0.052	A549	Lung carcinoma	Lung
	0.506	0.021	OVCAR-5	Ovarian adenocarcinoma	Ovarium
2940578	0.582	0.035	MCF 7.00	Breast carcinoma	Breast
24718647	0.415	0.032	NCI-H460	Non-small cell lung carcinoma	Lung
2924030	0.608	0.024	Hs 683	Oligodendroglioma	Brain
	0.513	0.018	NCI-H460	Non-small cell lung carcinoma	Lung
2940798	0.501	0.020	NCI-H460	Non-small cell lung carcinoma	Lung
2923908	0.583	0.030	Hs 683	Oligodendroglioma	Brain
	0.563	0.013	NCI-H460	Non-small cell lung carcinoma	Lung
	0.536	0.044	MCF 7.00	Breast carcinoma	Breast
4292821	0.543	0.015	NCI-H460	Non-small cell lung carcinoma	Lung
	0.507	0.051	MCF 7.00	Breast carcinoma	Breast
2949399	0.722	0.005	NCI-H460	Non-small cell lung carcinoma	Lung
	0.523	0.020	OVCAR-5	Ovarian adenocarcinoma	Ovarium
	0.510	0.034	DMS-114	Lung carcinoma	Lung
	0.509	0.050	MCF 7.00	Breast carcinoma	Breast
2923935	0.503	0.057	Hs 683	Oligodendroglioma	Brain
2949436	0.906	0.004	NCI-H460	Non-small cell lung carcinoma	Lung
	0.710	0.003	PANC-1	Pancreatic carcinoma	Pancreas
	0.704	0.004	ACHN	Papillary renal carcinoma	Kidney
	0.616	0.015	HCT-116	Colon carcinoma	Colon

3.5 Predicted Protein Targets and Biological Relevance of Indole Alkaloids

In addition to primary target prediction, *in silico* analysis was performed using PASS Targets to evaluate potential off-target interactions of the screened indole-alkaloid derivatives [25]. The predicted probabilities of activity (Pa) were used to assess the likelihood of compound–target associations, with Pa values of ≥ 0.70 considered high confidence, 0.50–0.69 as moderate confidence, and < 0.50 as low confidence [25]. Overall, the off-target prediction profile revealed a predominant association with serine/threonine kinase families, suggesting that structural features of the tested compounds may favor interactions with ATP-binding sites common to multiple kinases (Table 5 and Figure 5). Several compounds also showed predicted activity toward phosphoinositide kinases, GPCRs, and metabolic enzymes. Among the tested molecules, CID 4200841 exhibited a high-confidence off-target prediction for CaM kinase IV (Pa = 0.7070), along with moderate-confidence associations for dual specificity protein kinase CLK2 (Pa = 0.5677), endothelin receptor ET-A (Pa = 0.5642), serine/threonine-protein kinase PLK3 (Pa = 0.5608), and phosphatidylinositol-4-phosphate 3-kinase C2 domain-containing subunit gamma (Pa = 0.5287). The ET-A receptor interaction, in particular, could have cardiovascular implications if confirmed experimentally. CID 2949436 demonstrated the most extensive high-confidence kinase off-target profile, including Nek3 kinase (Pa = 0.8471) and PFTAIRE-2 kinase (Pa = 0.7630), as well as moderate-confidence predictions for phosphatidylinositol-4-phosphate 5-kinase type-1 gamma (Pa = 0.6357), PFTAIRE-1 kinase (Pa = 0.6200), and CaM kinase IV (Pa = 0.5117). This profile suggests a potential for multi-kinase activity that warrants in vitro selectivity evaluation. CID 2949399 also ranked highly for phosphatidylinositol-4-phosphate 5-kinase type-1 gamma (Pa = 0.7177) and Nek3 kinase (Pa = 0.6143), with additional predicted interactions involving rhodopsin kinase and homeodomain-interacting protein kinase 3. Meanwhile, CID 2940798 showed moderate predictions for MAP kinase ERK1 (Pa = 0.6042), microtubule-associated protein tau (Pa = 0.5441), cytochrome P450 2J2 (Pa = 0.5255), and CaM kinase IV (Pa = 0.5183), indicating possible effects on both cancer-related signaling and metabolic pathways. Several other compounds, including CIDs 2924030, 4292821, and 2923935, demonstrated moderate-confidence hits for CaM kinase IV, ERK1, and various mitotic kinases (e.g., NEK6, STK38-like, and BRK). In contrast, CIDs 2940578 and 2923908

exhibited only low-confidence predictions (Pa ~0.34–0.50), suggesting minimal off-target liabilities in the PASS model. The recurrence of CaM kinase IV as a predicted off-target across multiple scaffolds suggests specific structural motifs within the indole-alkaloid derivatives may mimic known ligands of this calcium/calmodulin-dependent kinase. Additionally, the frequent prediction of phosphoinositide kinases and NEK family members reflects a possible overlap in binding site compatibility with the ATP-binding region of Hsp90 NTD. While this could indicate polypharmacological potential, it also raises the need for kinase selectivity profiling during lead optimization. From a drug development perspective, the high Pa predictions for cancer-relevant kinases (e.g., ERK1, PLK3, Nek3) may offer opportunities for dual-targeting strategies, potentially enhancing anticancer efficacy. However, off-targets such as ET-A and CYP2J2 highlight the importance of early safety assessments to mitigate potential cardiovascular or metabolic adverse effects. Taken together, these findings underscore the necessity of integrating off-target prediction into the early stages of Hsp90 inhibitor development. The PASS-derived predictions provide a prioritized list of targets for follow-up validation using in vitro kinase assays, binding studies, and docking simulations. In particular, compounds such as CIDs 2949436, 2949399, and 4200841 merit focused investigation to confirm their selectivity profiles while harnessing their anticancer potential.

Table 5. Off-Target Predictions for Indole-Alkaloids Using PASS Targets Prediction Software

Compound CID	Target name	Confidence
4200841	CaM kinase IV	0.7070
	Dual specificity protein kinase CLK2	0.5677
	Endothelin receptor ET-A	0.5642
	Serine/threonine-protein kinase PLK3	0.5608
	Phosphatidylinositol-4-phosphate 3-kinase C2 domain-containing subunit gamma	0.5287
2940578	Serine/threonine-protein kinase OSR1	0.3435
	Hematopoietic cell protein-tyrosine phosphatase 70Z-PEP	0.3432
24718647	Eukaryotic translation initiation factor 4H	0.5656
	Polyadenylate-binding protein 1	0.5152
2924030	CaM kinase IV	0.5506
	MAP kinase ERK1	0.5225
2940798	MAP kinase ERK1	0.6042
	Microtubule-associated protein tau	0.5441
	Cytochrome P450 2J2	0.5255
	CaM kinase IV	0.5183
2923908	Serine/threonine-protein kinase OSR1	0.5022
4292821	CaM kinase IV	0.6184
2949399	Phosphatidylinositol-4-phosphate 5-kinase type-1 gamma	0.7177
	Serine/threonine-protein kinase Nek3	0.6143
	Rhodopsin kinase	0.5496
	Homeodomain-interacting protein kinase 3	0.5398
	cAMP-dependent protein kinase beta-1 catalytic subunit	0.5281
	Serine/threonine-protein kinase PFTAIRE-2	0.5063
2923935	Serine/threonine-protein kinase NEK6	0.5625
	Serine/threonine-protein kinase 38-like	0.5366
	Tyrosine-protein kinase BRK	0.5178
2949436	Serine/threonine-protein kinase Nek3	0.8471
	Serine/threonine-protein kinase PFTAIRE-2	0.7630
	Phosphatidylinositol-4-phosphate 5-kinase type-1 gamma	0.6357
	Serine/threonine-protein kinase PFTAIRE-1	0.6200
	Testis-specific serine/threonine-protein kinase 1	0.5867
	Serine/threonine-protein kinase tousled-like 1	0.5339
	Homeodomain-interacting protein kinase 3	0.5335
	cAMP-dependent protein kinase beta-1 catalytic subunit	0.5295
	CaM kinase IV	0.5117

Conclusion

This study highlights the important role of computer-aided drug discovery in identifying indole alkaloids as promising Hsp90 ATPase inhibitors. Using molecular docking and *in silico* profiling, these compounds showed strong binding affinities (–10.004 to –10.691 kcal/mol) and key interactions with catalytic residues Asp93, Lys58, Gly97, and Thr184. Computational ADME and toxicity predictions further confirmed their favorable drug-like properties, including compliance with medicinal chemistry filters, good solubility, moderate lipophilicity, high oral bioavailability, and no structural alerts. Notably, off-target interactions with kinases such as CaM kinase IV and Nek kinases indicate potential polypharmacological anticancer activity, though they also suggest a need to improve selectivity. Overall, this research demonstrates how computational methods can speed up the discovery of new chemotypes and help identify promising drug candidates. Supported by these *in silico* findings, indole alkaloids emerge as strong leads for developing Hsp90-targeted anticancer therapies, emphasizing the need for further mechanistic research and preclinical testing.

References

1. Jackson SE (2012) Hsp90: Structure and Function. pp 155–240
2. Wei H, Zhang Y, Jia Y, Chen X, Niu T, Chatterjee A, He P, Hou G (2024) Heat shock protein 90: biological functions, diseases, and therapeutic targets. MedComm (Beijing). https://doi.org/10.1002/mco2.470
3. Ciocca DR, Calderwood SK (2005) Heat shock proteins in cancer: diagnostic, prognostic, predictive, and treatment implications. Cell Stress Chaperones 10:86
4. Barrott JJ, Haystead TAJ (2013) Hsp90, an unlikely ally in the war on cancer. FEBS J 280:1381–1396
5. Keramisanou D, Aboalroub A, Zhang Z, Liu W, Marshall D, Diviney A, Larsen RW, Landgraf R, Gelis I (2016) Molecular Mechanism of Protein Kinase Recognition and Sorting by the Hsp90 Kinome-Specific Cochaperone Cdc37. Mol Cell 62:260–271
6. Aboalroub AA (2025) Pathogenic Proteins Through the Lens of NMR Spectroscopy: Structural and Functional Insights into Disease. Cell Biochem Biophys. https://doi.org/10.1007/s12013-025-01869-1
7. Bohush A, Bieganowski P, Filipek A (2019) Hsp90 and Its Co-Chaperones in Neurodegenerative Diseases. Int J Mol Sci 20:4976
8. Robbins N, Cowen LE (2023) Roles of Hsp90 in Candida albicans morphogenesis and virulence. Curr Opin Microbiol 75:102351
9. Poyya J, Joshi CG (2024) Inhibition of the HSP90 homodimerization and HSP90-HIF1α interactions by employing small molecules at C-terminal ATP binding site of HSP90. https://doi.org/10.1101/2024.06.02.595921
10. Keramisanou D, Vasantha Kumar MV, Boose N, Abzalimov RR, Gelis I (2022) Assembly mechanism of early Hsp90-Cdc37-kinase complexes. Sci Adv. https://doi.org/10.1126/sciadv.abm9294
11. Aboalroub A (2025) In Silico Identification of Spirodioxynaphthalenes as Promising Hsp90 Inhibitors. https://doi.org/10.21203/rs.3.rs-6199117/v1
12. Aboalroub AA (2025) Virtual Screening and Molecular Docking Characterization of Isoxazole-based Small Molecules as Potential Hsp90 Inhibitors: An in Silico Insight. Medinformatics. https://doi.org/10.47852/bonviewMEDIN52025019
13. Aboalroub AA, Al-Najjar BO (2024) In-silico identification of 3,4-Diarylpyrazoles-based small molecules as potential Hsp90 inhibitors. Results Chem 101757
14. Kitson RRA, Kitsonová D, Siegel D, Ross D, Moody CJ (2024) Geldanamycin, a Naturally Occurring Inhibitor of Hsp90 and a Lead Compound for Medicinal Chemistry. J Med Chem 67:17946–17963
15. Rosales PF, Bordin GS, Gower AE, Moura S (2020) Indole alkaloids: 2012 until now, highlighting the new chemical structures and biological activities. Fitoterapia 143:104558
16. de Sa Alves F, Barreiro E, Manssour Fraga C (2009) From Nature to Drug Discovery: The Indole Scaffold as a ‘Privileged Structure’ Mini-Reviews in Medicinal Chemistry 9:782–793
17. Dhyani P, Quispe C, Sharma E, et al (2022) Anticancer potential of alkaloids: a key emphasis to colchicine, vinblastine, vincristine, vindesine, vinorelbine and vincamine. Cancer Cell Int 22:206
18. Qin R, You F-M, Zhao Q, Xie X, Peng C, Zhan G, Han B (2022) Naturally derived indole alkaloids targeting regulated cell death (RCD) for cancer therapy: from molecular mechanisms to potential therapeutic targets. J Hematol Oncol 15:133
19. Lipinski CA (2004) Lead- and drug-like compounds: the rule-of-five revolution. Drug Discov Today Technol 1:337–341
20. HSP90 in complex with NVP-AUY922. https://doi.org/10.2210/pdb6lti/pdb
21. Morris GM, Huey R, Lindstrom W, Sanner MF, Belew RK, Goodsell DS, Olson AJ (2009) AutoDock4 and AutoDockTools4: Automated docking with selective receptor flexibility. J Comput Chem 30:2785–2791
22. Pettersen EF, Goddard TD, Huang CC, Couch GS, Greenblatt DM, Meng EC, Ferrin TE (2004) UCSF Chimera—A visualization system for exploratory research and analysis. J Comput Chem 25:1605–1612
23. Daina A, Michielin O, Zoete V (2017) SwissADME: a free web tool to evaluate pharmacokinetics, drug-likeness and medicinal chemistry friendliness of small molecules. Sci Rep 7:42717
24. Lagunin AA, Rudik A V., Pogodin P V., et al (2023) CLC-Pred 2.0: A Freely Available Web Application for In Silico Prediction of Human Cell Line Cytotoxicity and Molecular Mechanisms of Action for Druglike Compounds. Int J Mol Sci 24:1689
25. Lagunin A, Stepanchikova A, Filimonov D, Poroikov V (2000) PASS: prediction of activity spectra for biologically active substances. Bioinformatics 16:747–748
26. Li H, Sun X, Cui W, et al (2024) Computational drug development for membrane protein targets. Nat Biotechnol 42:229–242
27. Ekins S, Mestres J, Testa B (2007) *In silico* pharmacology for drug discovery: methods for virtual ligand screening and profiling. Br J Pharmacol 152:9–20
28. Brogi S, Ramalho TC, Kuca K, Medina-Franco JL, Valko M (2020) Editorial: In silico Methods for Drug Design and Discovery. Front Chem. https://doi.org/10.3389/fchem.2020.00612
29. Avendaño C, Menéndez JC (2023) Miscellaneous small- molecule and biological approaches to targeted cancer therapy. In: Medicinal Chemistry of Anticancer Drugs. Elsevier, pp 743–822
30. Röhrig UF, Goullieux M, Bugnon M, Zoete V (2023) Attracting Cavities 2.0: Improving the Flexibility and Robustness for Small-Molecule Docking. J Chem Inf Model 63:3925–3940

31. Gelis I, Keramisanou D, Aboalroub A (2017) Protein Kinase Recognition and Sorting by the HSP90 Kinome-Specific Cochaperone CDC37. Biophys J 112:491a
32. Kumar MV V, Ebna Noor R, Davis RE, Zhang Z, Sipavicius E, Keramisanou D, Blagg BSJ, Gelis I (2018) Molecular insights into the interaction of Hsp90 with allosteric inhibitors targeting the C-terminal domain. Medchemcomm 9:1323–1331
33. Reifs A, Fernandez-Calvo A, Alonso-Lerma B, et al (2024) High-throughput virtual search of small molecules for controlling the mechanical stability of human CD4. Journal of Biological Chemistry 300:107133
34. Eccles SA, Massey A, Raynaud FI, et al (2008) NVP-AUY922: A Novel Heat Shock Protein 90 Inhibitor Active against Xenograft Tumor Growth, Angiogenesis, and Metastasis. Cancer Res 68:2850–2860
35. Magwenyane AM, Lawal MM, Amoako DG, Somboro AM, Agoni C, Khan RB, Mhlongo NdumisoN, Kumalo HM (2022) Exploring the inhibitory mechanism of resorcinylic isoxazole amine NVP-AUY922 towards the discovery of potential heat shock protein 90 (Hsp90) inhibitors. Sci Afr 15:e01107
36. Pearl LH (2016) Review: The HSP90 molecular chaperone—an enigmatic ATPase. Biopolymers 105:594–607
37. Veber DF, Johnson SR, Cheng H-Y, Smith BR, Ward KW, Kopple KD (2002) Molecular Properties That Influence the Oral Bioavailability of Drug Candidates. J Med Chem 45:2615–2623
38. Shityakov S, Neuhaus W, Dandekar T, Förster C (2013) Analysing molecular polar surface descriptors to predict blood-brain barrier permeation. Int J Comput Biol Drug Des 6:146
39. Morak-Mlodawska B, Jelen M, Martula E, Korlacki R (2023) Study of Lipophilicity and ADME Properties of 1,9-Diazaphenothiazines with Anticancer Action. Int J Mol Sci 24:6970
40. Martin YC (2005) A Bioavailability Score. J Med Chem 48:3164–3170
41. Shin HK, Kang Y-M, No KT (2016) Predicting ADME Properties of Chemicals. In: Handbook of Computational Chemistry. Springer Netherlands, Dordrecht, pp 1–37
42. Shen J, Cheng F, Xu Y, Li W, Tang Y (2010) Estimation of ADME Properties with Substructure Pattern Recognition. J Chem Inf Model 50:1034–1041

Figures

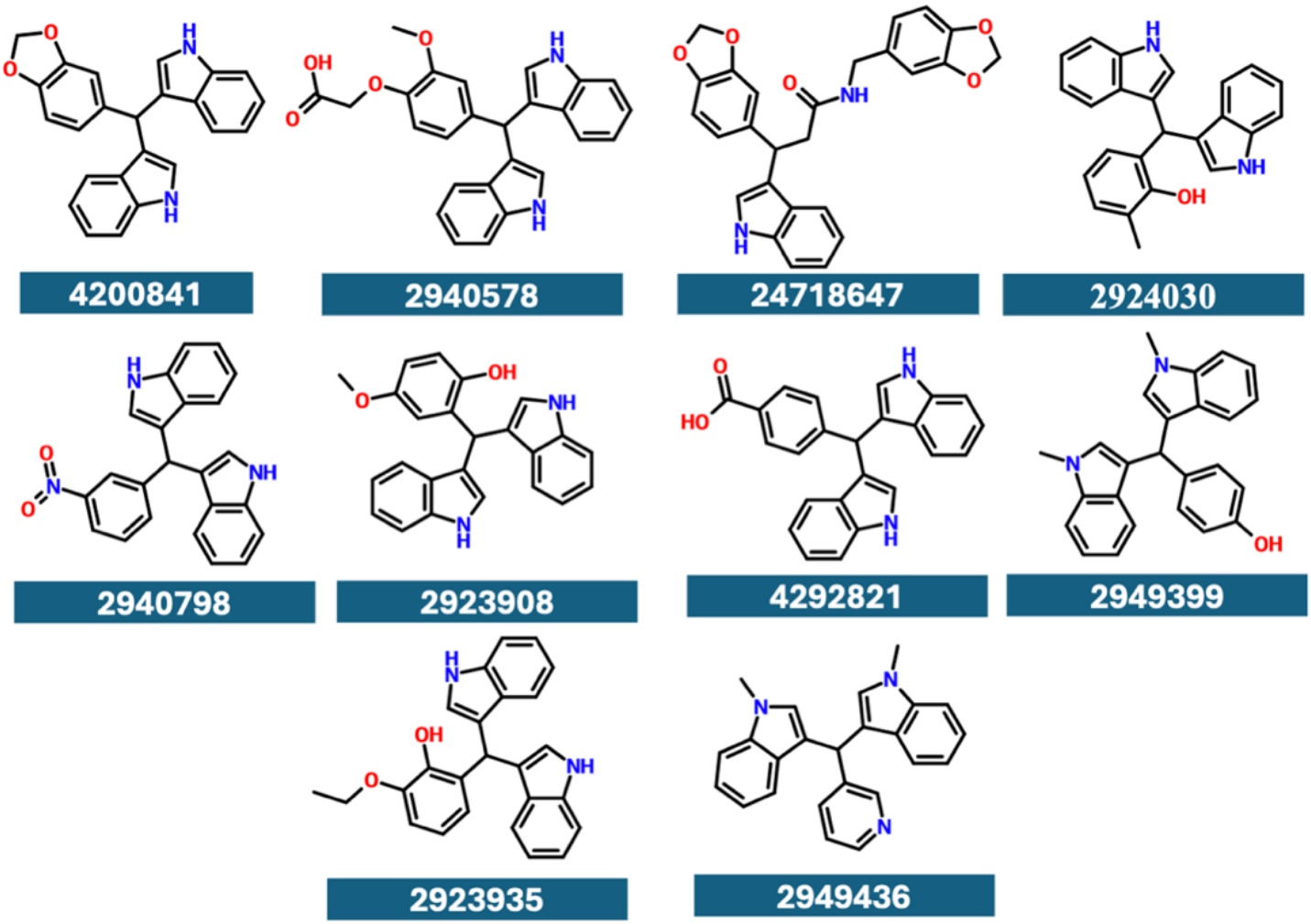

Figure 1

Chemical structures of the top 10 ranked indole alkaloid–based molecules docked into the Hsp90 ATP-binding site.

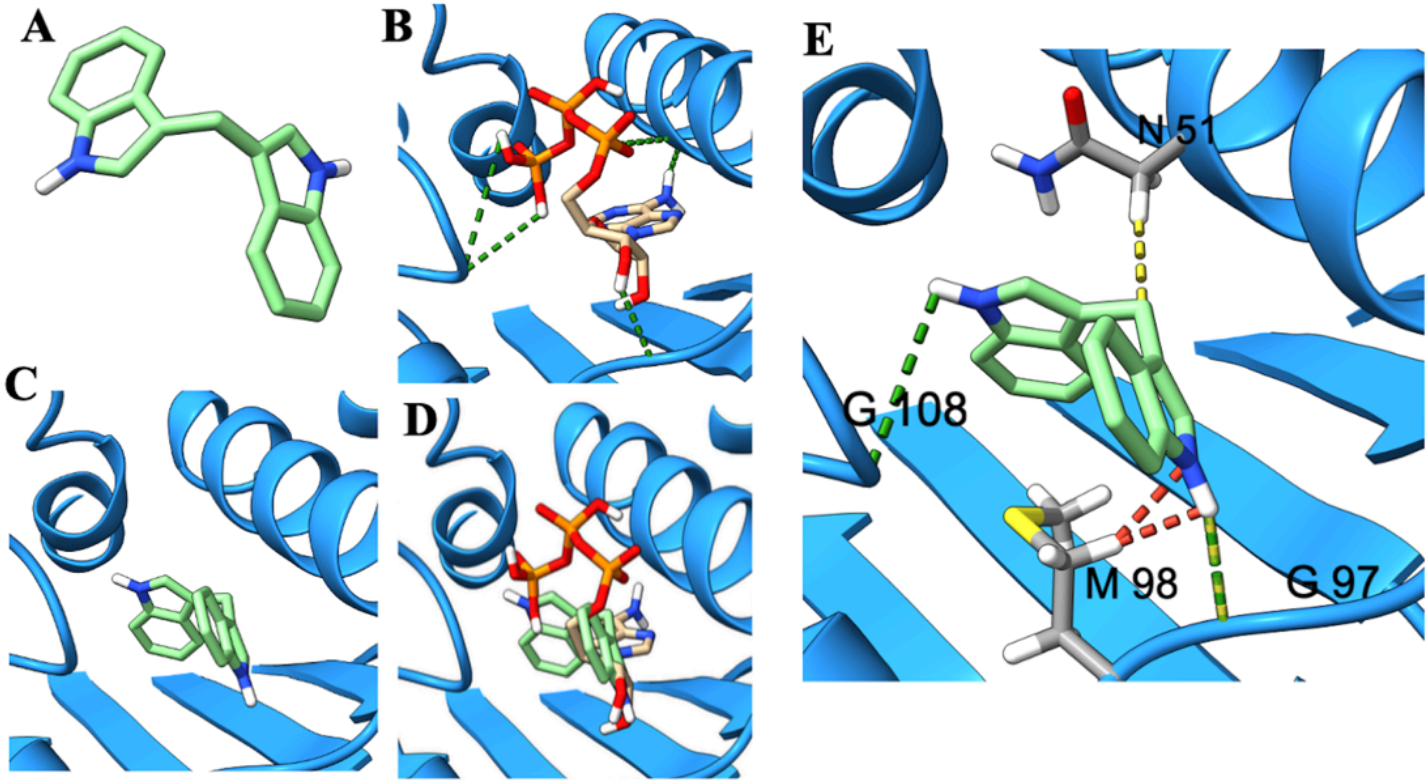

Figure 2

Structural and docking analysis of the 3,3'-di(indolyl)methane (DIM) scaffold in the Hsp90 N-terminal ATP-binding pocket. (A) General chemotype of identified hits, featuring a DIM-like scaffold. (B) ATP docking shows the adenine ring in the sub-pocket via hydrogen bonds (green), with the triphosphate moiety facing the solvent-exposed region. (C–D) Docked DIM occupies the same N-terminal ATP-binding pocket as ATP, with the aromatic core overlapping the adenine-binding region. (E) The quaternary carbon center orients the polyaromatic surface parallel to the hydrophobic wall of the pocket, enabling extensive contacts with surrounding residues.

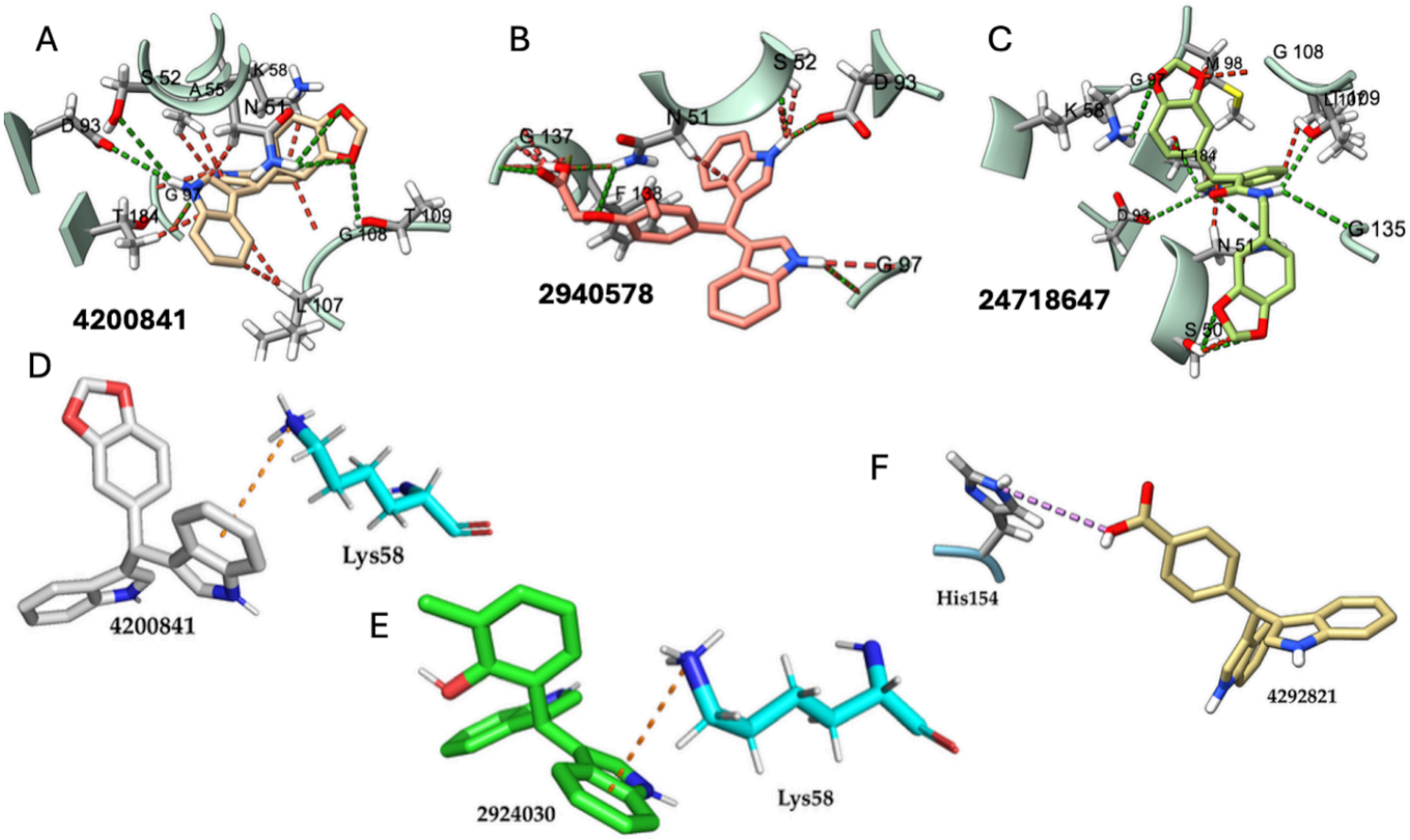

Figure 3

Interaction profile of the top-ranked indole alkaloids with Hsp90, showing hydrogen bonds (green) and hydrophobic contacts (red) within the ATP-binding pocket.

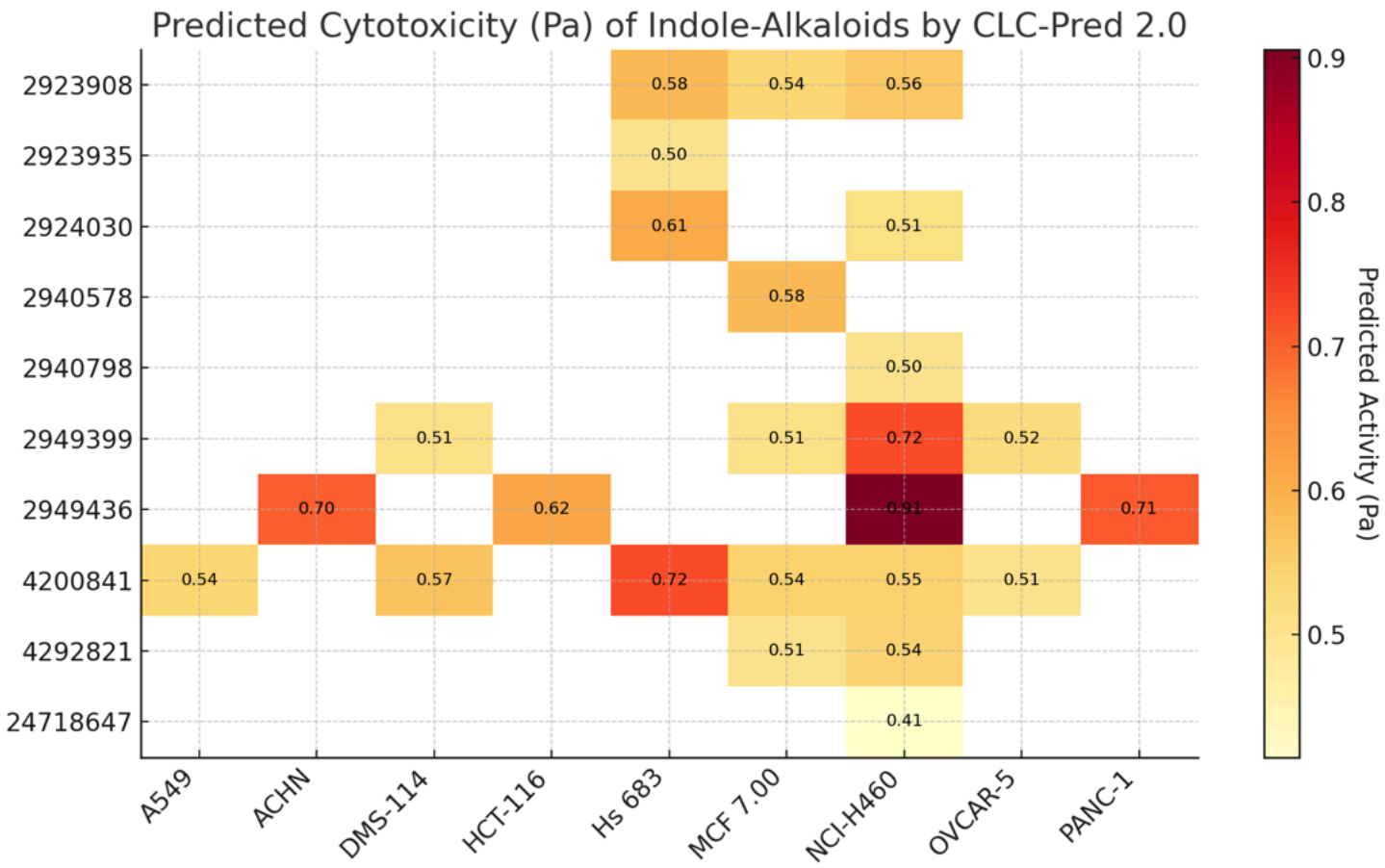

Figure 4

The heatmap of *in silico* cytotoxicity prediction of indole-alkaloids against cancer cell lines.

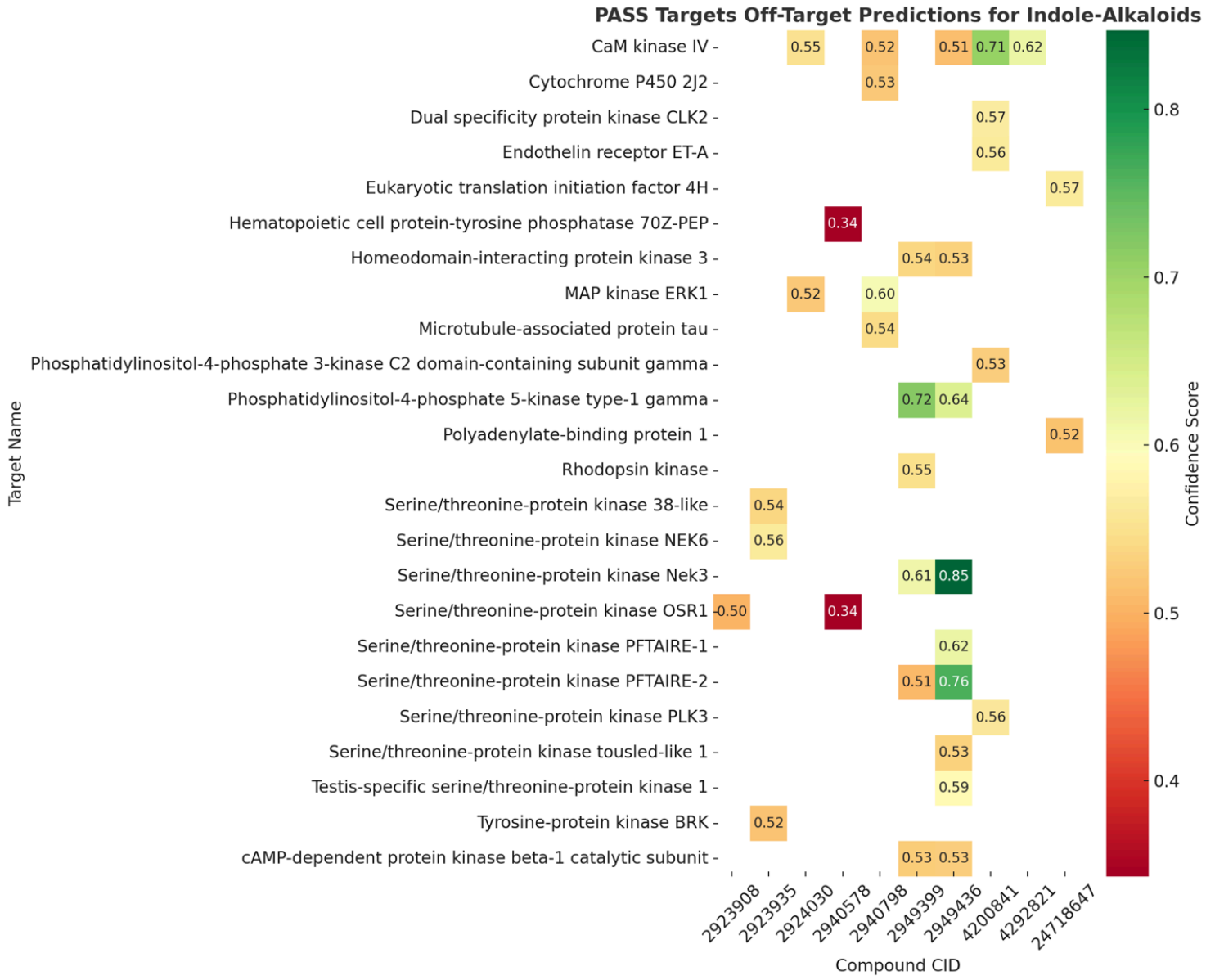

Figure 5

Predicted Off-Target Protein Interactions of Indole-Alkaloids Based on PASS Target Prediction